ISSN: 2230-9926

Available online at http://www.journalijdr.com

IJDR

International Journal of Development Research
Vol. 13, Issue, 08, pp. 63432-63437, August, 2023
https://doi.org/10.37118/ijdr.27051.08.2023

REVIEW ARTICLE OPEN ACCESS

APPLICATION FISCHER-TROPSCH SYNTHESIS: A REVIEW

***Jocielys Jovelino Rodrigues, Alfredina dos Santos Araújo, Josevânia Rodrigues Jovelino Torres, Filipe Tawâ Gomes, Antônio Fernandes Filho and Maria do Socorro Rodrigues Araújo**

Federal University of Campina Grande, Food Engineering Department

ARTICLE INFO

Article History:
Received 14th May, 2023
Received in revised form
28th June, 2023
Accepted 27th July, 2023
Published online 29th August, 2023

KeyWords:
SBA-15; Ruthenium; Rice husk ashes; Slurry bed reactor; Fischer-Tropsch synthesis.

****Corresponding author:***
Jocielys Jovelino Rodrigues

ABSTRACT

This work was to evaluate the catalytic properties Ru/Cobalt/SBA-15 catalyst for Fischer-Tropsch synthesis (FTS). The molecular sieve SBA-15 synthesized by hydrothermal method with rice husk ashes (RHA) and with tetraethyl orthosilicate (TEOS). The Ru promoted Co/SBA-15 catalyst was prepared by wet impregnation method and was characterized by X-ray diffraction, X-ray energy dispersion spectrophotometer, N_2 adsorption-desorption, temperature-programmed reduction and transmission electron microscopy. The Fischer-Tropsch synthesis using the catalysts were carried out to evaluate the catalysts activities and its effect on FTS product distribution. The synthesis was carried out in a slurry reactor operating at 513 K, 20 atm, CO : H_2 molar ratio of 1 : 2. X-ray diffraction showed that the calcined cobalt catalyst did not modify the structure of SBA-15, proving that Co was present under the form of Co_3O_4 in the catalyst. The addition of cobalt in SBA-15 decreased the specific superficial area of the molecular sieve. By RTP results was found the ranges of temperature reduction typical of iron oxides phases. Fischer-Tropsch synthesis activity and C_5^+hydrocarbon selectivity increased with the addition of Ru. The increases in activity and selectivity were attributed to the increased number of active sites resulting from higher reducibility and the synergetic effect of Ru and Co. The most interesting fact to be pointed out is that the use of this catalytic system for the catalyst prepared with alternative source of silica and cheap (rice hull ash) showed high selectivity in liquid products, that is, in hydrocarbons with C_5^+ (88.2% w/w), higher than the catalyst prepared with conventional silica source.

Citation: ***Jocielys Jovelino Rodrigues, Alfredina dos Santos Araújo, Josevânia Rodrigues Jovelino Torres, Filipe Tawâ Gomes, Antônio Fernandes Filho and Maria do Socorro Rodrigues Araújo. 2023.*** "Application fischer-tropsch synthesis: A review". *International Journal of Development Research*, 13, (08), 63432-63437.

INTRODUCTION

The technological and energetic development has been changing over the years, encouraging the search for new routes for fuel production, as well as the best use of existing technologies. The processes called XTL (X to liquid), where X represents the carbon source to be used, are routes capable of converting that carbon into liquid hydrocarbons. Generally, natural gas, coal and biomass can be used as the carbon source. The processes involving the conversion of natural gas into liquid are called gas-to-liquid (GTL), are also referred to as "Coal-to-liquid" (CTL) when using coal and biomass-to-liquid (BTL) when using biomass as a carbon source (Chen, 2018; Gavrilovic, 2018; Rytter, 2018 and Kliewer, 2018). Fischer-Tropsch synthesis is becoming a key industrial process in warranting a crude-oil independent supply of high quality liquid fuels, which fulfill the very stringent modern environmental requirements, by exploiting abundant and renewable sources such as natural gas and biomass. Fischer-Tropsch synthesis (FTS) is receiving renewed attention, driven by the global need to convert natural gas and nonpetroleum based energy resources into fuels and chemicals (Jiang, 2018; Steynberg, 2018; Lliuta, 2018l Zhang, 2018 and Phaahlamohlaka, 2018). The classical catalysts for the hydrogenation of CO are mainly Fe and Co. Cobalt-based catalysts promote higher yields, have a longer shelf life (less deactivation than iron catalysts) and have negligible activity for the reaction of Shift. The higher activity by weight of the metal, higher resistance to water deactivation and the lower production of oxygenates are advantages that the catalysts containing cobalt present against the iron-based catalysts. In order to improve the performance of these catalysts the so called promoters are generally used (Mangaloğlu, 2018; Rodrigues, Zhao, 1998 and Rodrigues, 2012). Cobalt is considered as the most favorable metal for the synthesis of long chain hydrocarbons due to its high activity, high selectivity to linear paraffins and low water-gas shift (WGS) activity. The use of SBA-15 as a support for cobaltbased FTS catalyst has been recently studied by several researchers (Rodrigues, 2012 and Ghampson, 2010). In recent years, various researches on materials used as catalyst support applied FTS have efficient results. Special emphasis has been given to the SBA-15, a silica-based mesoporous material with uniform hexagonal channels ranging from 3 to 30 nm, very narrow pore size distribution and high surface area (600–1000m^2/g) (Kliewer, 2018 and Jiang, 2018). Interestingly, SBA-15 also has thicker pore walls and better hydrothermal stability than MCM-41, a feature that can be relevant for the FTS process because water is an by-product (Rodrigues, and Zhao, 1998 and Rodrigues, 2012). Xiong *et al*. (Xiong, 2010) have prepared highly dispersed Co/SBA-15 catalysts. The addition of a small amount of Ru promoter to Co/SBA-15 has decreased the reduction temperature of both reduction steps (Co3O4→CoO and CoO→Co^0) and suppressed the formation of Co^{2+}

species. With increasing ruthenium content, catalyst reducibility increased and the surface enriched in cobalt atoms. The raw material normally used as the source of Si for the synthesis of the SBA-15 molecular sieve is TEOS (tetraethylorthosilicate). The silica source can be selected through criteria such as availability, chemical reactivity and cost. Molecular sieves produced from alternative sources of silica is presented as a promising technology as it replaces the conventional silica source of high financial value (TEOS) for alternative sources of silica (RHA) and these sources are found in abundance, and is the raw material of low cost. Silica obtained from rice husk have been used with great success as a raw material for producing catalysts, demonstrating its high technological potential. However, the use of silica in catalysis requires, in most cases, purification processes for the removal of minor components present. These processes involve, in general, heat treatment and acid (Rodrigues, Loy, 2018; Nicodeme, 2018 and Chen, 2018). The objective of this work was to investigate the effect of ruthenium promoter on Co/SBA-15 (TEOS and RHA) catalyst in Fischer-Tropsch synthesis. In this work, a slurry reactor operating under typical industrial conditions was used to assess the performance of the catalyst in the Fischer-Tropsch synthesis.

Experimental

Preparation of SBA-15: SBA-15 was synthesized according to the procedure reported in the literature. First, 2 g Pluronic P123 (Aldrich) was dissolved in 12 g deionized water and 59 g 2 mol/L HCl solution while stirring. Then, 4.20g silica source was added into the solution while stirring. This mixture was stirred continuously for 24 h. The gel mixture was then transferred to a Teflon-lined autoclave and kept static at 365 K for two days. The productwas centrifuged at 11000 rpm, washed with deionized water several times and dried at 373 K. The material was calcined in static air at 820 K for 1 h to remove the polymer template and to obtain white SBA-15 powder. The sample was synthesized with the following molar composition: 1.0 Silica source: 0.016 P123: 5.6 HCl: 191 H2O.

Preparation of Co/SBA-15 and Ru/Co/SBA-15 catalysts: Four catalysts were prepared: the Co/SBA-15 catalyst (used as control catalyst) and the Ru/Co/SBA-15 catalyst. Co/SBA-15 (TEOS and RHA) catalyst was prepared containing 20 % (w/w) Co and Ru/Co/SBA-15 (TEOS and RHA) catalyst was prepared containing 0.5 % (w/w) Ru and 20% (w/w) Co. The deposition of metal with 20 % (w/w) Co on SBA-15 support was carried out by wet impregnation. 0.1 mol/L aqueous solution of cobalt nitrate [$Co(NO_3)_2 \cdot 6H_2O$] was used to deliver the amount of cobalt to the support. The impregnation was carried out at room temperature for 35 min under continuously stirring. The mixture was dried at 353 K for 24 h. The solid material was calcined at 472 K under a nitrogen flow rate of 100 mL/(gcat·min), with a heating ramp of 280 K/min starting from room temperature, and kept at the final temperature for 1 h. After this period, the nitrogen flow was replaced by synthetic air and the sample was heated again at 275 K/min from 472 K to 723 K, and kept at this temperature for 2 h. Ru/Co/SBA-15 catalyst was prepared by co-impregnation of SBA-15. First, 0.1 mol/L aqueous solution of cobalt nitrate [$Co(NO_3)_2 \cdot 6H_2O$] was used to deliver the amount of cobalt to the support. Afterwards, the impregnation of Ru was carried out using an aqueous solution of ruthenium-nitrosyl. Ru/Co/SBA-15 catalyst was calcined using the same procedure described for the production of Co/SBA-15 (Rodrigues and Rodrigues, 2012).

Characterization of samples

X-ray energy dispersion spectrophotometer (EDX): Elemental analysis was determined through energy dispersive Xray spectrophotometry, in a Shimadzu EDX-700 instrument.

X-ray diffraction (XRD): Powder diffraction patterns were measured on a Shimadzu XRD 6000. The average diameter of the sample crystallites was determined by Scherre equation.

Analysis by temperature-programmed reduction (TPR): Calcined samples were characterized by TPR using a Micrometrics ChemiSorb 2720 instrument under a mixed H_2-N_2 flow (5% H_2 at 30 mL/min).

Nitrogen adsorption (BET method): The textural characteristics of the catalyst were investigated by isothermal gas adsorption/desorption of N_2 at 77 K using a Micrometrics equipment. The adsorption and desorption N_2 isotherms were obtained in the range of relative pressure (p/p_0) between 0.02 and 1.0. The values of the average pore diameter and surface area (SBET) were obtained by the proposed method (BET).

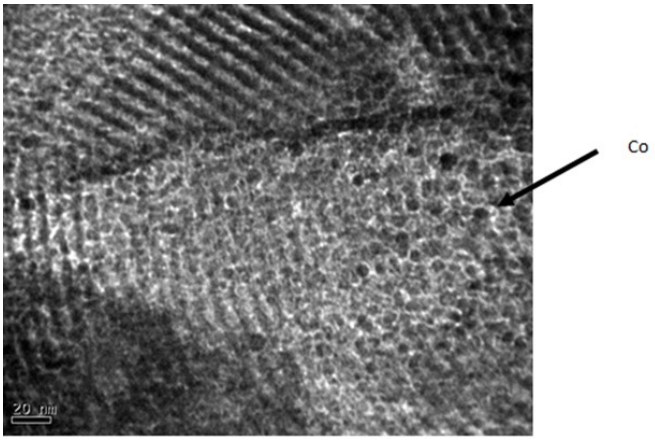

Transmission electron microscopy (TEM): The analyses were performed on JEOL equipment Model JEM-1200 EX II Instrument with the technique of embedding in Araldite resin and then cut with Sorvall MT 5000 ultramicron.

Fischer-Tropsch Synthesis: The Fischer-Tropsch Synthesis (FTS) was carried out in a stirred, semi-batch 500 mL autoclave reactor. The reaction was carried out with 2 grams of catalyst suspended in 150 mL of hexadecane in a high-pressure autoclave reactor (Parr Instruments model 4571). The hexadecane was inert under the present reaction conditions. Tests were carried out at a total pressure 20 atm, 513 K (optimal condition for catalyst performance) with a H_2:CO feed ratio of 1:1 [11,12]. The synthesis gas was prepared by mixing H_2 and CO through two mass flow controllers (Alborg GFC-17), enabling the desired H_2/CO ratio to be obtained. The feed was introduced into the reactor below the agitator. The reaction was conducted under constant mechanical agitation (800 rpm) [11], and a gas entrainment impeller was used to provide constant recirculation of the syngas to the slurry phase. The catalytic experiments the catalysts were reduced in situ at atmospheric pressure done before the addition of hexadecane by increasing the temperature at a heating rate of 1 K/min up to 673 K and maintained at this temperature for 10 h while passing a flow of pure hydrogen (400 cm^3/min) through the reactor (Figure 1).

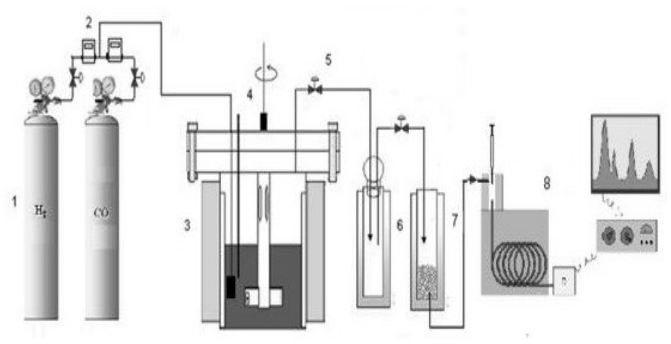

Figure 1. Scheme of the reaction system used to carry out the Fischer-Tropsch reaction. 1. Gas cylinders; 2. Flow controllers; 3. Reactor; 4. Gas entrainement impeller and magnetic drive; 5. Outlet control valve; 6. High temperature trap; 7. Low temperature water trap; 8. Gas chromatograph.

The reason for the reducing Co at very low heating rate (ten hours and in excess of hydrogen) is cobalt oxide more difficult to reduce. This can be seen in the literature [13]. After the reduction step the temperature was lowered to 373 K under the flow of H_2 and then the reactant gas mixture (H_2:CO) was introduced at a total flow rate of 250 cm^3/min (H_2/CO = 1), corresponding to a GHSV of 13.5l (NTP)/(g_{cat} h) referred to the syngas feed, and the reactor pressure slowly increased up to 20 bar. Then, the temperature in the catalyst bed was increased from 373 to 513 K at a controlled heating rate of 4 K/min in order to avoid instability of the system induced by the highly exothermic. The Fischer-Tropsch Synthesis (FTS) was carried out in a stirred, semi-batch 500 mL autoclave reactor. The reaction was carried out with 3 grams of catalyst suspended in 150 mL of hexadecane in a high-pressure autoclave reactor (Parr Instruments model 4571). The hexadecane was inert under the present reaction conditions. Tests were carried out at a total pressure 20 atm, 513 K (optimal condition for catalyst performance) with a H_2:CO feed ratio of 1:1 [11,12]. The synthesis gas was prepared by mixing H_2 and CO through two mass flow controllers (Alborg GFC-17), enabling the desired H_2/CO ratio to be obtained. The feed was introduced into the reactor below the agitator. The reaction was conducted under constant mechanical agitation (800 rpm) [6], and a gas entrainment impeller was used to provide constant recirculation of the syngas to the slurry phase (Figure 1). The analysis of the products of the FTS was obtained after 6 h mass balance periods (after steady state was reached), allowing the accumulation of the liquid products in the reactor. The gas and liquid phase products were analyzed in a Gas chromatograph (Model Thermos Ultra), equipped with thermal conductivity (TCD) and flame-ionization (FID) detectors. Temperature programming (303 K to 573 K) with an OV-1 capillary column (30 m × 0.25-mm i.d. × 0.25-μm film) allowed the identification of Fischer-Tropsch products (C_1 to C_{40}). The conversion of syngas into hydrocarbons was determined by mass balance of CO, assayed using the same temperature programming with a Supelco Q-Plot capillary column (30 m × 0.25-mm i.d. × 0.25-μm film). A microcomputer used for performing data acquisition and process control also controlled automatic chromatograph sampling. The FTS product distribution was determined by mass balance of carbon species, which has considered the conversion of syngas and the mass fractions of hydrocarbon species in the gas and liquid phases.

XRD. This shows that by dissolving the Pluronic P123 driver in water and hydrochloric acid under stirring and heating (35 °C) the copolymer /solvent interactions are formed. After addition of the silica source, silica /solvent interactions are formed to then form the silica / copolymer interactions. The gel obtained when subjected to the aging process for 24 h under agitation may result depending on the conditions of the solution (temperature, pH) in a siloxane phase by the condensation of the silica species on the micelles directing the copolymer, and thus, the gel can be subjected to a hydrothermal treatment to increase the thickness of the silica wall, forming the SBA-15 molecular sieve as verified by Figures 2 and 3 (Rodrigues, 2012 and Cai, 2008). X-ray diffraction profiles did not change significantly after impregnation with Co and co-impregnation with Ru. X-ray diffraction profiles presented high diffraction peaks showing that SBA-15 has maintained its ordered structure after impregnation with cobalt and ruthenium Figure 4 and 5 (TEOS) and Figure 6 and 7 (RHA). Cobalt nitrate is transformed into cobalt oxide during calcination under synthetic air environment (Mendes, 2006). At temperatures above 473 K, cobalt nitrate decomposed releasing NOx and Co^{2+} ions were converted into Co_3O_4, as reported by Chen *et al*. (2008) and Ghampson *et al*. (2010). The presence of peaks indicating the formation of Co_3O_4 species in Co/SBA-15 catalyst was identified using JCPDS-ICDD li brary (International centre for diffraction data). The presence of peaks at Co_3O_4 (2θ = 31,3°; 36,9°; 45,1°; 59,4° e 65,4°).

$$d = \frac{0.89\lambda}{B\cos\theta}.\frac{180°}{\pi} \quad (1)$$

where, d is the cobalt particle diameter, λ is the X-ray wave length (1.54056 A), and ˚ B is the full width half maximum of Co diffraction peak. The chemical composition of SBA-15 and the catalysts are presented in Table 1. The support and the catalysts have presented high levels of silica (SiO_2), which was expected because the structure of SBA-15 molecular sieve consists solely of silica. After impregnation of cobalt on SBA-15 at a 20 % (w/w) nominal level of cobalt, it was possible to verify the presence of cobalt oxide (Co_3O_4) in the samples. The average crystallite sizes of Co_3O_4 are presented in Table 2.

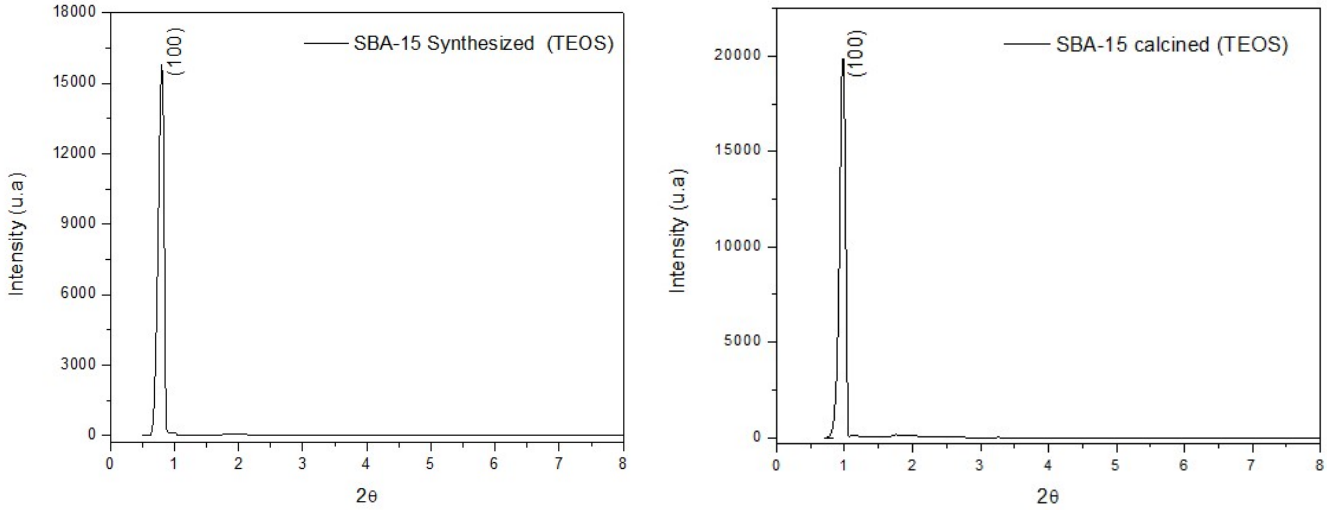

Figure 2. Diffractogram of synthesized and calcined SBA-15 (TEOS)

RESULTS AND DISCUSSION

The X-ray diffraction profiles at samples (SBA-15 synthesized and calcined) obtained with TEOS and RHA are shown in Figures 2 and 3, respectively. It can be observed pattern formation characteristic of the structure of a hexagonal symmetry typical p6mm SBA-15 (Zhao, 1998; Rodrigues, 2012; Martinez, 2003 and Cai, 2008). The main diffraction peak, with Miller index of (1 0 0), referring to the crystal planes, characteristic of this type of material can be observed by

The crystallite diameter decreased slightly with the addition of Ru, indicating that Ru have facilitated the dispersion of Co_3O_4 on the catalyst surface (Rodrigues, 2012 and Martinez, 2003). The textural analysis of the calcined SBA-15 support and the catalysts is presented in Table 3. The specific area and total specific pore volume of the calcined SBA-15 molecular sieve given in Table 3 are typical of SBA-15 structures synthesized under similar conditions (Rodrigues, 2012). The incorporation of cobalt in the support resulted in a sharp decrease in surface area. This decrease may be attributed to the dilution effect of the support caused by the presence of the supported

cobalt oxide phase, and in a minor extent to a partial blockage of the support pores (especially micropores and mesopores) (Rodrigues, Gonzalez, 2009 and Mendes, 2006).

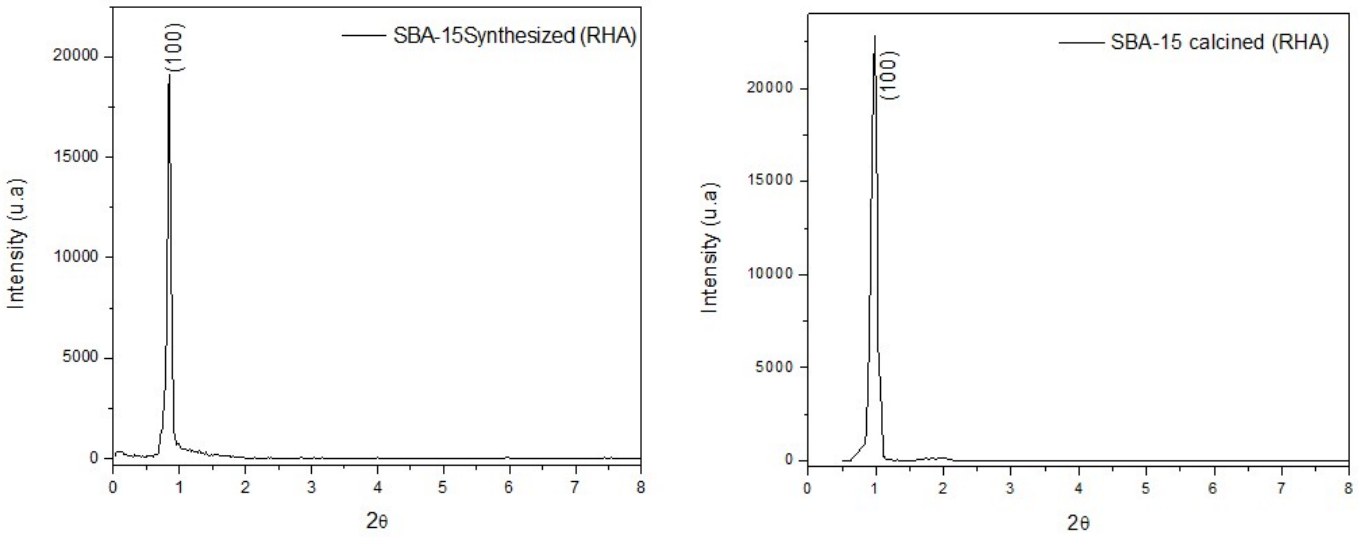

Figure 3. Diffractogram of synthesized and calcined SBA-15 (RHA)

Table 1. Chemical composition of SBA-15 and catalysts

Samples	SiO_2	Co_3O_4	Co	Impurities
20% (w/w) Co/SBA-15 (TEOS)	71.10	28.30	20.1	0.6
20% (w/w) Co/0.5% (w/w) Ru/SBA-15(TEOS)	71.00	27.30	19.4	1.7
20% (w/w) Co/SBA-15 (RHA)	68.45	29.35	20.9	2.2
20% (w/w) Co/0.5% (w/w) Ru/SBA-15 (RHA)	68.20	28.96	21.3	2.8

Table 2. Average sizes of crystallites

Catalysts	Averagecrystallitesize (nm)
20% (w/w) Co/SBA-15 (TEOS)	18.5
20% (w/w) Co/0.5% (w/w) Ru/SBA-15(TEOS)	11.1
20% (w/w) Co/SBA-15 (RHA)	20.6
20% (w/w) Co/0.5% (w/w) Ru/SBA-15 (RHA)	12.2

Table 3. Textural analysis of the calcined SBA-15 calcined and catalysts

Samples	S_{BET} (m^2/g)	V_{Ptotal}(cm^3/g)
20% (w/w) Co/SBA-15 (TEOS)	440	0.72
20% (w/w) Co/0.5% (w/w) Ru/SBA-15(TEOS)	381	0.70
20% (w/w) Co/SBA-15 (RHA)	459	0.69
20% (w/w) Co/0.5% (w/w) Ru/SBA-15 (RHA)	339	0.63

Table 4. Catalytic performance of 20% (w/w) Co/SBA-15 and 20% (w/w)Co/0.5% (w/w) Ru/SBA-15 catalysts in a slurry reactor for Fischer-Tropsch synthesis

Catalysts	XCO (%)	C_1-C_4	C_5^+
20% (w/w) Co/SBA-15 (TEOS)	35	26.5	70.5
20% (w/w) Co/SBA-15 (RHA)	36	27.6	72.4
20%(w/w) Co/0.5% (w/w) Ru/SBA-15 (TEOS)	40	18.5	81.5
20%(w/w) Co/0.5% (w/w) Ru/SBA-15 (RHA)	40	11.8	82.2

Figures 8, 9 and 10 show the N_2 adsorption/desorption isotherms at 77 K of the calcined SBA-15 and catalysts. The isotherms for the calcined SBA-15 sample were of type IV and have exhibit a well-defined H1 hysteresis loop according to the IUPAC classification relative to the mesoporous materials. There is also a H1 hysteresis phenomenon characterized by two branches of quasi-vertical and parallel isotherms over a wide range of ordinate values (adsorbed quantity). When comparing the SBA-15 molecular sieve isotherm obtained with RHA with that synthesized with TEOS, it is verified that there are no significant differences that could disclose the type IV isotherm and type H1 hysteresis characteristic of mesoporous materials. There is only a slight difference between the inflection obtained for the SBA-15 (RHA), which was between 0.60-0.77 while the SBA-15 (TEOS) showed inflection between 0.47-0.79, however these ranges of values are within the values observed in the literature for SBA-15 prepared with conventional reagent (TEOS) (Ghampson, 2010; Martinez, 2003). The isotherms for the catalysts showed similar profiles, typically of type IV.

The desorption curve for this catalyst also showed an H1 hysteresis loop for partial pressures (p/p_0) between 0.6 and 0.8, which can be attributed to capillary condensation and evaporation in the internal mesoporous structure of the tubes (Rodrigues, 2012; Ghampson, 2010; Martinez, 2003). TPR profiles of the catalysts catalysts 20% (w/w) Co/SBA-15 (TEOS) and 20 %(w/w) Co/SBA-15 (RHA) are shown in Figure 11. Analyzing the RPT profile of the catalyst 20% (w/w) Co/SBA-15 (TEOS), it was found that this catalyst presented reduction peaks located approximately of 398K and 615K can be attributed to the reduction of Co_2O_3 in two phases (Co_2O_3 => CoO => Co^0). The peak located at approximately 657K is related to the reduction of cobalt oxide (Co^{2+} and CO^{3+}) species, which interact with the support and are difficult to reduce (Rodrigues, 2012; Gonzalez, 2009; Cai, 2008). The 20%(w/w) Co/SBA-15 (RHA) catalyst showed the first localized reduction peak at approximately

482K, and this temperature is higher than that presented by the Co/SBA-15 (TEOS) catalyst, probably this may have occurred due to interactions between metal-support. In the second stage of reduction, the behavior similar to the Co/SBA-15 (TEOS) catalyst was observed, with a peak located at approximately 630K, corresponding to the CoO => Co^0 reduction. Similarly, the peak located at approximately 668K occurs due to interactions of metal species with the support (Rodrigues, 2012 and Cai, 2008). Noble metals can be reduced at temperatures lower than cobalt oxides. Thus, in its metallic state, the noble metals tend to favor the dissociation and the activation of the H_2 and, in this way, benefit the cobalt reduction process (Xiong, 2010; Gonzalez, 2009 and Cai, 2008). TPR profiles of the catalysts 20% (w/w) Co/0.5%(w/w) SBA-15 (TEOS) and 20 20% (w/w)Co/0.5% (w/w) SBA-15 (RHA) are shown in Figure 12. For the catalyst 20% (w/w) Co/0.5%(w/w) SBA-15 (TEOS), although there was no decrease in the temperature of reduction of Co_3O_4 species for CoO, it was evident the decrease in temperature to obtain Co^0. In the second stage the temperature of reduction of this species decreased significantly from 615 K to 557K. It is observed that ruthenium favors the reduction of Co_3O_4 to CoO, reducing the temperature of reduction of this species from 482K to 433K, as can be seen in the first reduction peak. In the second stage the reduction temperature of this species decreased significantly from 630K to 553K.

It is also verified that the presence of ruthenium in the catalyst favored the elimination of the peak of hydrogen consumption located approximately between 657- 668K, indicating that ruthenium favors the reduction of the interaction between cobalt oxide species (Co^{2+} and CO^{3+}) and the support (SBA-15) and thus facilitated the reduction of these cobalt species that are difficult to reduce (Rodrigues, ? & 2012). Representative TEM images of the catalysts 20% (w/w) Co/SBA-15 (TEOS) and 20% 20% (w/w) Co/SBA-15 (RHA) catalysts, respectively, are shown in Figures 13 and 14. In both cases, many agglomerations formed by spherical cobalt species with a size of 20 nm were observed. It is also verified that on the edges the cobalt particles are irregular. It has also been observed that cobalt particles with smaller diameters are dispersed in the support, while larger ones agglomerate on the outer surface. The interplanar distances of these particles were 0.150 nm, which is related to cobalt oxide (CoO). With these results, it can be stated that the diameter of the cobalt particles supported in SBA-15 is influenced by the pore diameter of the mesoporous silica, especially when it comes to samples prepared by wet impregnation, where size control does not occur (Rodrigues, 2012). Generally, metal fillers with high contents of the active phase on the catalytic supports tend to decrease the dispersion of the metal, forming large agglomerates of the metal particles. This process can be further aggravated if there is a low interaction between the metal phase and the carrier, thus increasing the mobility of the particles and, consequently, favoring the formation of metal particle agglomerates. No significant morphological changes were observed between Co/SBA-15 (TEOS) and Co/SBA-15 (RHA) catalysts. TEM images of the catalysts 20% (w/w) Co/0.5% (w/w) Ru/SBA-15 (TEOS) and 20% (w/w) Co/0.5% (w/w) Ru/SBA-15 (RHA) after reduction are shown in Figure 15 and 16 respectively. In contrast, the addition of ruthenium as a promoter of the catalytic system tends not to promote the formation of large clusters with a defined shape. Thus, it was observed that the addition of ruthenium increased the dispersion of the cobalt particles, reducing the size of the metal particles to 10 nm. This was verified for both catalysts 20% (w/w) Co/0.5% (w/w) Ru/SBA-15 (TEOS) and 20% (w/w) Co/0.5% (w/w) Ru/SBA-15 (RHA). This occurs due to the intervention of ruthenium in the precursor kinetics of the precursor, altering the nucleation and crystallization of the cobalt oxide species and favoring the formation of smaller particles (Rodrigues, Rodrigues, 2012 and Cai, 2008). The performance of the catalyst in FT synthesis is presented in Table 4. The catalyst with Ru promoter has presented a lower methane selectivity and higher C_5^+ hydrocarbon selectivity. The conversion of syngas into hydrocarbons has increased slightly with the addition of ruthenium to the catalyst (Rodrigues, 2012). The results of catalyst activity in terms of syngas conversion (X_{CO}) and selectivity in terms of hydrocarbon product distribution (C_1 to C_5^+, in %), after 6 hours of reaction with the 20 % (w/w) Co/0.5 % (w/w) Ru/SBA-15 catalyst, are shown in Table 4. As can be verified from the results the catalyst 20% (w/w) Co/SBA-15 (TEOS) presented average conversion of 35%, the catalyst 20% (w/w) Co/SBA-15 (RHA) obtained average conversion of 36% and as expected 20%(w/w) Co/0.5% (w/w) Ru/SBA-15 (TEOS) and 20%(w/w) Co/0.5% (w/w) Ru/SBA-15 (RHA) catalysts were obtained after the introduction of the promoter. This high conversion of the synthesis gas can be explained because the regular mesoporous structure has a beneficial effect on the mass transfer. The carrier chosen should allow the oxide species to be reduced in the presence of hydrogen but at the same time that there is a certain interaction that ensures the maintenance of the size distribution of metal particles on the surface of the carrier. The overall conversion of CO appears to be related to the access of the reactants, while the selectivity relates to the olefin reinsertion capacity, which is directly linked to the metal-support interaction. Thus, an optimized catalyst would be one that can aggregate these two characteristics (Rodrigues & Rodrigues, 2012).

According to FURTADO *et al*., (Furtado, 2013), the catalytic activity is linear to the loading of Co in the catalytic system employed in the Fischer-Tropsch synthesis, high metal contents lead to greater activities, which can be attributed to increase of active sites. This allows to assume that the metal dispersion did not undergo significant variations with the increase of the metal content in the catalyst. Diffusion problems with reactants and products during the reaction may

decrease activity and selectivity in long-chain hydrocarbons during Fischer-Tropsch synthesis. It is observed from the results presented that the selectivity in liquid hydrocarbons, for all the catalysts, is distributed in a very similar way. The catalysts 20% (w/w) Co/SBA-15 (TEOS) obtained selectivities around 26.5% for the C1-C4 range and 73.50 for the C_5^+ range. The 20% (w/w) Co/SBA-15 (RHA) catalyst presented values of selectivities around 27.61% was obtained for the C1-C4 range and 73.39% for the C_5^+ range. However, an increase in the selectivity for the C5 + fraction can be noted when the catalytic system was promoted with ruthenium. It is also observed that the introduction of ruthenium detracts from the production of hydrocarbons with chains between 1 and 4 carbons, mainly in the production of methane which is the primary and undesirable product of the Fischer-Tropsch reaction. The concentration of metal in the catalyst can influence the distribution of C_5^+ hydrocarbons. The selectivity in the fraction between C5 and C12 is favored by a higher cobalt concentration, which can be attributed to the increase in the number of active sites (Rodrigues, Rodrigues, 2012 and Furtado, 2013). However, the most interesting fact to be pointed out is that the use of this catalytic system for the catalyst prepared with an inexpensive and cheap silica source (rice hull ash) showed high selectivity in liquid products, that is, in hydrocarbons with C_5^+ and the formation of oxygenated products in this reaction was not verified. The catalyst 20% (w/w) Co/0.5% (w/w) Ru/SBA-15 (RHA) showed selectivity for the C_5^+ range around 82%. The performance of this catalyst may have been due to the presence of ruthenium as catalyst promoter, where it favored the reduction of cobalt species in the presence of hydrogen, assisted its dispersion as well as increased the selectivity of C_5^+ hydrocarbons.

CONCLUSIONS

The material obtained by the hydrothermal method using rice husk ashes as silica source showed typical features of SBA-15 molecular sieve, with a structure that includes multi-level mesopores, crystallites, and grains within the original particles. When cobalt is incorporated into the support, the properties of the final catalyst thereby prepared are close to theoretical values, demonstrating the efficiency of the wet impregnation technique. With the addition of Ru, the activity of a catalyst for FT synthesis increased due to increased reducibility of the catalyst and the synergistic effect between Ru and Co. The crystallite diameter decreased slightly with the addition of Ru, indicating that Ru has facilitated the dispersion of Co_3O_4 on the catalysts. The decrease in C1-C4 selectivity and the higher C_5^+ hydrocarbon selectivity are caused by the decrease of Co^{2+}

and Co^{3+} species on the catalyst surface with the addition of ruthenium. However, the most interesting fact to be pointed out is the use of this catalytic system for the catalyst prepared with alternative and cheap silica source showed high selectivity in liquid products, that is, in hydrocarbons with C_5^+ chains and no formation of products was verified oxygenated in this reaction. The 20% (w/w) Co/0.5% (w/w) Ru/SBA-15 catalyst showed selectivity for a C_5^+ range around 88.2%. The performance of this catalyst may have been due to the presence of ruthenium as catalyst promoter, where it favored a reduction of cobalt species in the presence of hydrogen, assisted its dispersion as well as increase the selectivity of C_5^+ hydrocarbons.

REFERENCES

Cai Q, Li J. Catal Commun, 2008, 9: 2003

Chen G, Li J, Cheng Z, Yan B, Yao *J. Appl Energy*, 2018, 217: 249-257

Chen W, Lin Y, Daí Y, Na Y, Sun Y. Catal Today, 2018, 311: 8-22.

D, Zhao; Q, Huo; J, B, F, Fend; G, D, Chmelka. *J Am Chem Soc,* 1998, 120, 6024-6036.

Furtado J L B, Carvalho A, Vieira R. Advanced Chem Letters, 2013, 1: 317-320

Gavrilovic L, Brandin J, Holmen A, Venvik H, Blekkan E. Appl Catal B, 2018, 230: 203-209.

Ghampson I T, Newman C, Konk L, Pier E, Hurley K D, Pollock R A, Walsh B R, Goundie B, Wright J, Wheeler M C, Meulenberg R W, Desisto W J, Frederick B G, Austin R N. Appl Catal A, 2010, 388: 57

Gonzalez O, Perez H, Navarro P, Almeida L C, Pacheco J G, Montes M. Catal Today, 2009, 148:140.

J, J, Rodrigues; Fernandes; M, G, F, Rodrigues. Applied Catalysis A General 21, 722-728.

J, J, Rodrigues; G, Pecchi; F, A, N, Fernandes; M, G, F, Rodrigues. *J Nat Gas Chem,* 2012, 21, 722-728.

Jiang Z, Zhao Y, Huang C, Song Y, Liu Z. Fuel, 2018, 226: 213-220.

Kliewer C E, Soled S L, Kiss G. Catal Today In press, 2018.

Lliuta I, Larachi F. Chem Eng Sci, 2018, 177: 509-522

Loy A C M, Yusup A, Lam M K, Chin N L F, Acda M N. Energy Conv Manag, 2018, 165: 541-554

Mangaloğlu D U, Baranak M, Atac O, Atakul H. J Ind Eng Chem, 2018, in press.

Martinez A, López C, Márquez F, Díaz I. J Catal, 2003, 220: 486

Mendes F M T, Perez C A C, Noronha F B, Souza C D D, Cesar D V, Freund H J, Schmal M. *J Phys Chem* A, 2006, 110: 9155

Nicodeme T, Barchem T, Jacquet N, Richel A. Renew Sust Energy Rewiews, 2018, 88:151-159

Phaahlamohlaka T N, Dlamini M W, Mogodi M W, Kumi D O, Coville N J. Appl Catal A, 2018, 552: 129-137.

Rytter E, Borg Ø, Tsakoumis N, Holmen A. *J Catal,* 2018, 365: 334-343

Steynberg A, Deshmukh S, Bobota H. Catal Today, 2018, 299: 10-13

Xiong K, Li J, Liew K, Zhan X. Appl Catal A, 2010, 389:173

Zhang X, Qian W, Zhang H, Sun Q, Ying W. Chin J. Chem Eng, 2018, 26: 245-251

****